

Enzyme Inhibition | Hot Paper |

Phosphono Bisbenzguanidines as Irreversible Dipeptidomimetic Inhibitors and Activity-Based Probes of Matriptase-2

Daniela Häußler,^[a] Martin Mangold,^[a] Norbert Furtmann,^[a, b] Annett Braune,^[c] Michael Blaut,^[c] Jürgen Bajorath,^[b] Marit Stirnberg,^[a] and Michael Gütschow^{*,[a]}

Abstract: Matriptase-2, a type II transmembrane serine protease, plays a key role in human iron homeostasis. Inhibition of matriptase-2 is considered as an attractive strategy for the treatment of iron-overload diseases, such as hemochromatosis and β -thalassemia. In the present study, synthetic routes to nine dipeptidomimetic inactivators were developed. Five active compounds (**41–45**) were identified and characterized kinetically as irreversible inhibitors of matriptase-2. In addition to a phosphonate warhead, these dipeptides possess two benzguanidine moieties as arginine mimetics to provide affinity for matriptase-2 by binding to the S1 and S3/S4 subpockets, respectively. This binding mode was strongly supported by covalent docking analysis. Compounds **41–45**

were obtained as mixtures of two diastereomers and were therefore separated into the single epimers. Compound **45A**, with *S* configuration at the N-terminal amino acid and *R* configuration at the phosphonate carbon atom, was the most potent matriptase-2 inactivator with a rate constant of inactivation of $2790 \text{ M}^{-1} \text{ s}^{-1}$ and abolished the activity of membrane-bound matriptase-2 on the surface of intact cells. Based on the chemotyp of phosphono bisbenzguanidines, the design and synthesis of a fluorescent probe (**51A**) by insertion of a coumarin label is described. The in-gel fluorescence detection of matriptase-2 was demonstrated by applying **51A** as the first activity-based probe for this enzyme.

Introduction

The cell-surface protease matriptase-2, encoded by the *TMPRSS6* gene, is a member of the type II transmembrane serine proteases. The family members exhibit a short intracellular N-terminal tail, a transmembrane domain, and a large extracellular portion containing a variable stem region and a C-terminal serine protease catalytic domain with a highly conserved chymotrypsin fold. Matriptase-2 belongs to the trypsin-like proteases, which preferentially cleave substrates with arginine or lysine in the P1 position.^[1,2]

Matriptase-2 has attracted strong attention because of its contribution to the regulation of iron homeostasis. It has been found that mutations in the *TMPRSS6* gene cause iron-refractory iron deficiency anemia (IRIDA) in humans and an anemic

and iron-deficient phenotype in murine models.^[3] Matriptase-2 is expressed mainly in hepatocytes and it negatively regulates the production of hepcidin, the systemic iron-regulatory hormone. Hepcidin regulates cellular iron export by promoting the degradation of the iron transporter ferroportin.^[4] The expression of *HAMP*, the gene of hepcidin, is controlled through the bone morphogenetic protein/son of mothers against decapentaplegic (BMP/SMAD) pathway as follows. An activated complex, composed of the BMP receptor, its endogenous ligand BMP6, and the coreceptor hemojuvelin phosphorylates the SMAD1/5/8–SMAD4 complex, which then causes increased expression of *HAMP*. The presence of intact hemojuvelin is required for this signaling cascade^[5] and, accordingly, causes limited iron absorption and iron release.^[4] Matriptase-2 exerts its influence as a regulator of this pathway by hydrolytically cleaving hemojuvelin from the plasma membrane, which leads to a down-regulation of *HAMP* expression. Putative cleavage sites in hemojuvelin have been suggested after arginine residues.^[5,6] These cleavage sites correspond to the primary substrate specificity of matriptase-2 to hydrolyze a peptide bond after basic amino acids, with a preference for arginine over lysine, in the P1 position.^[2] Matriptase-2 undergoes complex autoprocessing that results in activation and release from the cell surface, as shown in a transfected cell system.^[7] These autoprocessing sites also feature a P1 arginine residue. Attempts to develop peptidic substrates for matriptase-2 revealed that, in addition to the P1 arginine, further basic amino acids at positions P4–P2 are favored,^[8] which was confirmed by a combinatorial approach that identified the preferred P4–P1 substrate sequence

[a] D. Häußler, M. Mangold, N. Furtmann, Dr. M. Stirnberg, Prof. Dr. M. Gütschow
Pharmaceutical Institute, Pharmaceutical Chemistry I
University of Bonn, An der Immenburg 4, 53121 Bonn (Germany)
E-mail: guetschow@uni-bonn.de

[b] N. Furtmann, Prof. Dr. J. Bajorath
Department of Life Science Informatics, B-IT
LIMES Program Unit Chemical Biology and Medicinal Chemistry
University of Bonn, Dahlmannstrasse 2, 53113 Bonn (Germany)

[c] Dr. A. Braune, Prof. Dr. M. Blaut
Department of Gastrointestinal Microbiology
German Institute of Human Nutrition Potsdam-Rehbruecke
Arthur-Scheunert-Allee 114–116, 14558 Nuthetal (Germany)

Supporting information for this article can be found under <http://dx.doi.org/10.1002/chem.201600206>.

as Ile–Arg–Ala–Arg.^[9] So far, the characterization of the (patho)-physiological role of matriptase-2 has been hampered by the lack of specific antibodies and activity-based probes.

Matriptase-2 is involved in disease states related to human iron homeostasis. Mutations in the *TMPRSS6* gene lead to IRIDA, a rare autosomal recessive disorder.^[10] Matriptase-2 emerges as a potentially important pharmaceutical target for the treatment of iron-overload diseases, based on the consideration that inhibition of matriptase-2 activity increases *HAMP* expression and, accordingly, attenuates the plasma iron level.^[11,12] Hereditary hemochromatosis and β -thalassemia represent prominent examples of iron-overload diseases. It has been shown in mouse models of hereditary hemochromatosis or β -thalassemia that iron overload can be prevented by targeting *TMPRSS6*. The β -thalassemia mouse model mimics non-transfusion-dependent thalassemia conditions that are associated with a suppression of *HAMP*. In both models, the treatment of such mice with *TMPRSS6* small interfering RNA diminishes iron overload by up-regulation of hepcidin expression.^[13] Similarly, an antisense oligonucleotide strategy was pursued, which demonstrated decreased serum iron, transferrin saturation, and iron accumulation in the liver of mice affected by hereditary hemochromatosis and an improved anemia in β -thalassemia mice.^[14] Therefore, selective, low-molecular-weight matriptase-2 inhibitors might be beneficial as pharmacological tools to investigate further the exact role of the protease in regulating iron homeostasis and, moreover, as leads for the therapeutic treatment of iron-overload diseases, in particular, the iron overload in thalassemic patients receiving multiple blood transfusions.^[4,11,12]

For this study, we considered peptidomimetic phosphonates as potential inhibitors of matriptase-2. The irreversible mode of action is based on nucleophilic attack of the active-site serine and the simultaneous release of one phenolic residue. The resulting serine phosphono diester might undergo a slow aging upon loss of the second phenoxy group to form a phosphono monoester. An advantage of phosphonates compared with other classes of inhibitors is a complete lack of activity against cysteine or threonine proteases.^[15] Covalent inhibitors might have several potential benefits, such as 1) improved biochemical efficiency of target disruption, 2) prevention of drug resistance, and 3) more stable pharmacokinetics.^[16] However, irreversible inhibitors could also modify off-targets and may lead to a risk of organ toxicity because such electrophiles are able to react with circulating nucleophiles, for example, glutathione.^[17]

To attain sufficient potency and the desired selectivity of phosphonate inhibitors for a trypsin-like serine protease, their structures might advantageously be equipped with residues of basic amino acids at the P1 position or with other positively charged groups, such as amidines or guanidines.^[18–26] Beside their utilization as arginine mimetics, benzamidine and benzguanidine moieties have been successfully introduced into anti-protozoal and antifungal compounds.^[27] In certain cases, their fluorescent properties have been shown to depend on the insertion into the minor groove of double-strand DNA.^[28] For our design of matriptase-2 inhibitors, the introduction of an arginine mimetic was intended to enable an interaction with the

deep S1 pocket of the target enzyme.^[11,29,30] Beside the ionic interaction in the S1 binding pocket, an additional positively charged moiety of an inhibitor should be able to interact with the upper part of the S3/S4 binding pocket of matriptase-2, where the backbone carbonyl oxygen atoms of Glu662, Asp663, and Ser664 provide a negatively charged environment.^[11,29,30] Among the few peptidomimetic inhibitors reported for matriptase-2 so far, the presence of two basic substructures turned out to be favorable.^[11,29,31] In particular, this was the case for a series of peptidyl benzothiazole ketones, for which the following P4–P1 sequences afforded the most potent inhibitors of matriptase-2: Arg–Gln–Tyr–Arg, Trp–Cys–Tyr–Arg, Arg–Gln–Phe–Arg, and Lys–Trp–Trp–Arg.^[32] The presence of a second basic amino acid in three of these sequences supported the design of dibasic inhibitors for matriptase-2 and was in agreement with the preferred aforementioned P4–P1 substrate sequences.^[7,8]

Protein profiling with activity-based probes has emerged as a powerful strategy to study enzyme functions and activities in complex proteomes.^[20,21,33–35] The visualization of the target is restricted to the active form of the enzyme, which is of particular importance, because enzyme expression levels do not always correlate with the activity or the activity might be regulated post-translationally.^[34,36] These probes consist of three essential components: a reactive group, a recognition element, and a reporter tag. The reactive group, a so-called warhead, leads to a covalent attachment to an active-site nucleophile. Electrophilic moieties applied for serine protease probing comprise fluorophosphonates, diphenylphosphonates, sulfonyl fluorides, and isocoumarins.^[35]

Results and Discussion

We aimed at synthesizing dipeptidomimetic inhibitors for matriptase-2 with the following structural features. An aminophosphonate moiety in place of the C-terminal amino acid was supposed to act as a warhead and enable irreversible inhibition of the target protease. In addition, two arginine-mimetic substructures would be introduced for an attractive interaction with the S1 and S3/S4 subsites: one guanidinophenyl group as an α -substituent at the aminophosphonate and an N-terminal guanidinobenzoyl capping group (Figure 1). Our synthetic strategy involved the construction of the entire phosphono dipeptide, followed by the generation of the guanidine moieties from the nitro groups of the precursors. Five points of diversity were planned to be introduced, that is, the position of the guanidine group at both benzguanidines, the nature (and ste-

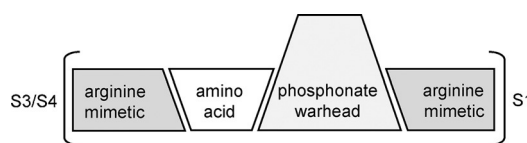
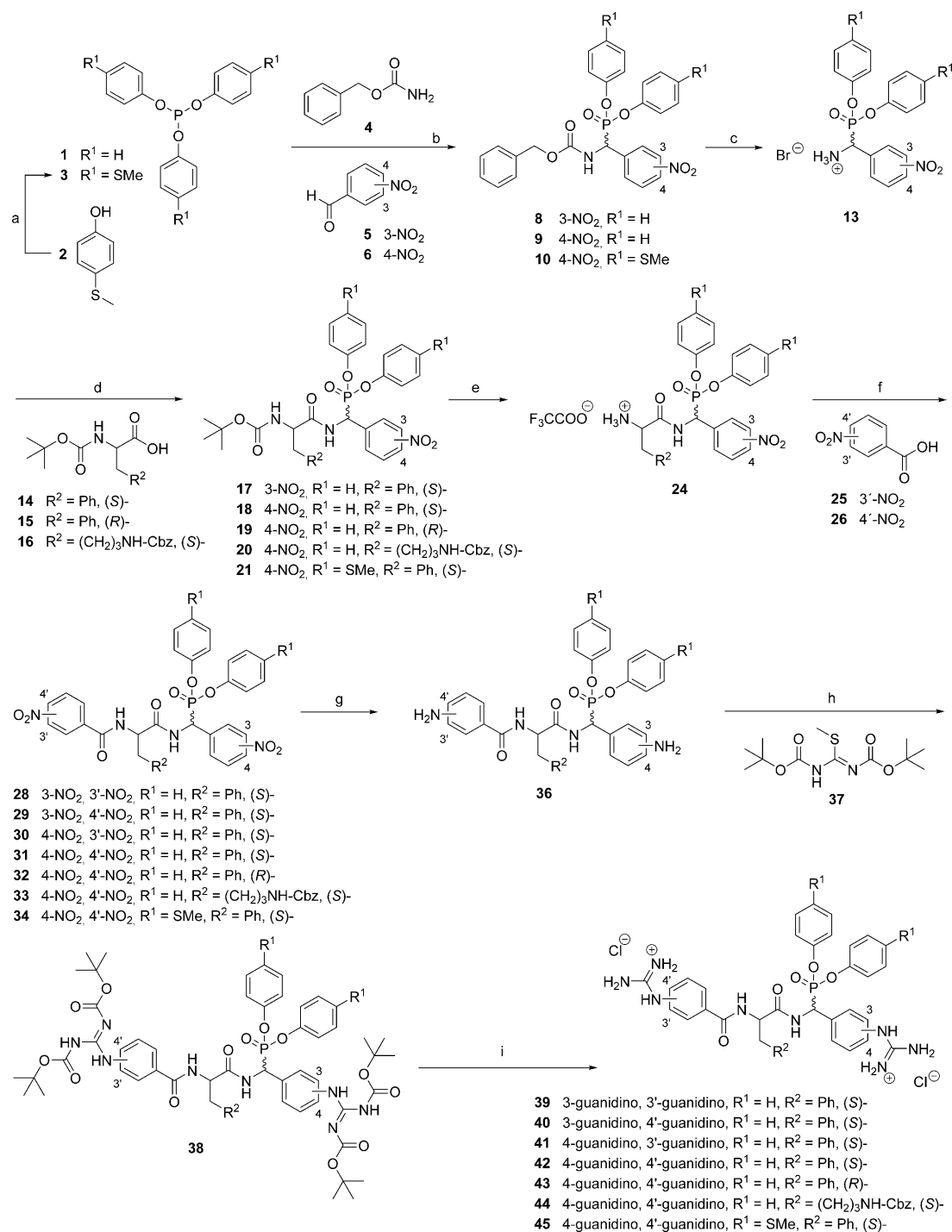


Figure 1. Schematic composition of the phosphono bisbenzguanidines described herein.

reochemistry) of the N-terminal amino acid, and the O substituents at the phosphonate moiety.

Scheme 1 outlines the eight-step synthetic approach toward the bisguanidine phosphonates **39–45**. The linear synthesis started with the Oleksyszyn reaction, a three-component reaction to obtain the α -aminophosphonate building block.^[18,37] This transformation involved a phosphite (**1** or **3**), benzyl car-

bamate (**4**), and an aldehyde. Either 3-nitrobenzaldehyde (**5**) or 4-nitrobenzaldehyde (**6**) was used to introduce structure diversity. Whereas triphenylphosphite (**1**) was commercially available, tris(4-(methylthio)phenyl)phosphite (**3**) was synthesized by heating PCl_3 with 4-(methylthio)phenol (**2**) in acetonitrile at reflux.^[19,38,39] The Cbz-protected aminophosphonates **8–10** were obtained as racemic mixtures in good yields. Deprotec-



Scheme 1. Synthesis of compounds **39–45**. Reaction conditions: a) PCl_3 , MeCN, reflux; b) AcOH, 90 °C; c) AcOH/HBr, RT; d) HATU, DIPEA, DMF, RT; e) TFA, CH_2Cl_2 , RT; f) HATU, DIPEA, DMF, RT; g) $\text{SnCl}_2 \cdot 2\text{H}_2\text{O}$, H_2O , EtOAc, reflux; h) HgCl_2 , TEA, CH_2Cl_2 , RT; i) TFA, CH_2Cl_2 , RT, prep. HPLC, HCl, lyophilization. Cbz: benzyl-oxycarbonyl; HATU: *N*-[[(dimethylamino)-1*H*-1,2,3-triazole[4,5-*b*]-pyridin-1-ylmethylene]-*N*-methylmethanaminium hexafluorophosphate; DIPEA: diisopropylethylamine; TFA: trifluoroacetic acid; TEA: triethylamine.

tion of the amino group was achieved after treatment with a solution of HBr in acetic acid.^[20,21,33,37,38,40] The bromide salts **13** were directly subjected to a coupling reaction with the amino acids Boc-L-Phe-OH (**14**; Boc: *tert*-butoxycarbonyl), Boc-D-Phe-OH (**15**), and Boc-L-Lys(Cbz)-OH (**16**), respectively, by applying HATU as coupling reagent and DIPEA as base.^[21,33,41] Other guanidinium/uronium coupling reagents or carbodiimides have also been employed for the preparation of several phosphono dipeptides.^[18,20,22,24,33,38,42] The resulting Boc-protected peptides **17–21** occurred as a mixture of two diastereomers after the introduction of a second chiral center, which originated from the introduced amino acid.

In order to remove the Boc protecting group, compounds **17–21** were treated with trifluoroacetic acid to obtain the ammonium salts **24**. To insert a further point of diversity, the free amine was coupled with either 3-nitrobenzoic acid (**25**) or 4-nitrobenzoic acid (**26**). For this purpose, the protocol with HATU and DIPEA was reapplied to yield the bisnitro compounds **28–34**. For the subsequent reduction of the nitro groups, SnCl₂ acted as the reducing agent.^[19,26] In accordance with a previously described method,^[19,20,26] the so-obtained aniline derivatives **36** were converted into protected guanidines in a HgCl₂-promoted reaction with *N,N'*-di-Boc-*S*-methylisothiourea (**37**) and Et₃N. Somewhat different approaches have been reported for phosphonates with Boc-protected benzguanidine moieties performing the aniline guanylation with *N,N'*-di-Boc-1-guanylpiperazine,^[23,24] or *N,N'*-di-Boc-2-(trifluoromethylsulfonyl)guanidine.^[21] The desired guanidine phosphonates **39–45** were obtained after removing the Boc protecting groups with trifluoroacetic acid in dichloromethane.^[19] Afterwards, the products were purified by means of preparative HPLC and lyophilization to give the final hydrochloride salts **39–45**.

In addition to the phosphonate diphenyl esters **39–44** and the bismethylthiophenyl ester **45**, a compound was designed in which the aryloxy moieties were exchanged for ethoxy groups. Its structure, **46**, is shown in Table 1. The preparation of **46** is depicted in Scheme S1 in the Supporting Information. The transesterification of diphenyl phosphonates constitutes one efficient route to dialkyl phosphonates.^[43] Thus, with the diphenyl phosphonate **9** (structure in Scheme 1) as the starting material, a Cbz-protected α -amino diethyl phosphonate was prepared in ethanol in the presence of KF/18-crown-6 ether.^[33,43] By following a route analogous to that described above, via the corresponding mononitro and bisnitro intermediates, the guanidine phosphonate diethyl ester **46** was achieved. For this exemplary synthesis, the substitution pattern of **42** was chosen by taking the bioactivity data of the phenoxy derivatives into account (see below). With consideration of previous results on the inhibition of human thrombin and bovine trypsin by peptide phosphonate derivatives,^[18] a diethyl substitution at the phosphorus was not expected to cause an improved potency. Nevertheless, it was intended to verify this at matriptase-2.

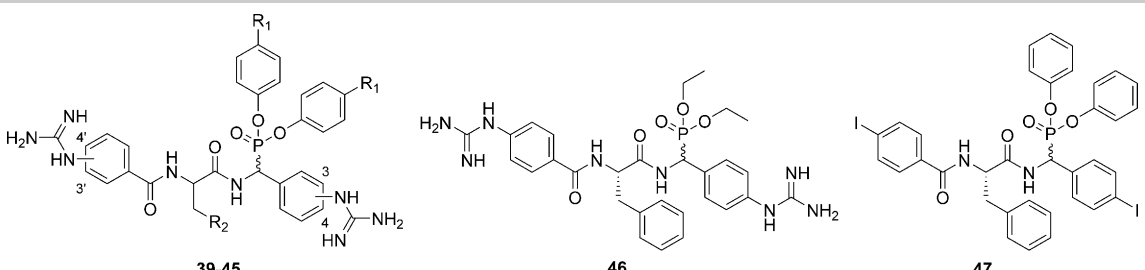
It has been reported that positively charged groups (e.g., guanidines, amidines) of protein ligands can be exchanged for halogen atoms that are able to perform protein–ligand interactions in so-called halogen bonding.^[44] Accordingly, compound

47 (see Table 1 for its structure), a bisiodine phosphonate analogue of **42**, was synthesized (Scheme S2 in the Supporting Information). The general synthetic approach to the protected α -aminophosphonates was performed with 4-iodobenzaldehyde to place the iodine at the P1 residue. After Cbz deprotection, coupling to Boc-L-Phe-OH (**14**), and Boc deprotection, the second iodine functionality was introduced by using 4-iodobenzoic acid.

The phosphono dipeptides **39–47** were evaluated at matriptase-2 and three related serine proteases, that is, human thrombin, bovine factor Xa, and bovine trypsin; selected compounds were also evaluated at human trypsin. These enzymes were assayed with fluorogenic peptide substrates and the reactions were followed over 30 min. The active compounds were measured at five different inhibitor concentrations and the progress curves were analyzed. In most cases, the active compounds exhibited a time-dependent inhibition; non-linear regression of the progress curves provided pseudo-first-order rate constants of irreversible inhibition, k_{obs} . These k_{obs} values were then plotted versus the inhibitor concentrations and the parameters for the inactivation (k_{inac}/K_i) were calculated from the second-order rate constants, $k_{\text{obs}}/[I]$, obtained by linear regression. The results of the kinetic experiments are summarized in Table 1.

Initially, the influence of the positions of the guanidine moieties on the inhibitory activity toward matriptase-2 was investigated. We compared compounds **39**, **40**, **41**, and **42**, which possess a different guanidino substitution pattern but share the remaining structural features. Whereas a *meta* substitution at the “Eastern” part (position 3) led to inactive compounds (**39**, **40**), a guanidine group in the *para* position (position 4) was advantageous (**41**, **42**) and, in combination with a *para* substitution at the “Western” part (position 4'), gave a k_{inac}/K_i value of $120 \text{ M}^{-1} \text{ s}^{-1}$ for the inactivation of matriptase-2 by compound **42**. The guanidino substitution pattern clearly affected the selectivity of the phosphono bisbenzguanidines **39–42**. A *meta* substitution at the “Eastern” part (position 3) caused inhibition of thrombin, whereas matriptase-2, factor Xa, and bovine trypsin were not affected by **39** and **40**. Unexpectedly, the inhibition of thrombin was not time dependent. Rates in the presence of different inhibitor concentrations were determined from linear regression of the progress curves to obtain IC₅₀ values, which are unsuitable for a comparison with the second-order rate constants of inactivation. The influence of the substrate concentration on thrombin inhibition by **39** was analyzed and revealed a noncompetitive mode of inhibition (see Figure S1 in the Supporting Information). Further studies might clarify the inhibition of thrombin by **39** and **40** and address the question of to what extent the phosphonate moiety might be involved in the enzyme–inhibitor interaction. As *para*-guanidine groups at the “Eastern” (position 4) and “Western” part (position 4'), as present in **42**, were beneficial for matriptase-2 inhibition, this substitution pattern was kept in the other phosphono dipeptides of this study (**43–47**). These compounds did not inhibit either thrombin or factor Xa, but the inactivation of matriptase-2 (by **42–45**) was generally accompanied by inactivation of bovine trypsin. We also deter-

Table 1. Inhibition of serine proteases by phosphono dipeptides **39–47**.



Comp.	Positions of the guanidine residues	Compound ^[a]	R ¹	R ²	Enzyme inactivation, k_{inac}/K_i [$\text{M}^{-1} \text{s}^{-1}$] ^[b,c]			
					Human matriptase-2	Human thrombin	Bovine factor Xa	Bovine trypsin
39 (<i>S, rac</i>)	3'	3	H	Ph	n.i.	$\text{IC}_{50} = (1.66 \pm 0.12) \mu\text{M}$ ^[d]	n.i.	n.i.
40 (<i>S, rac</i>)	4'	3	H	Ph	n.i.	$\text{IC}_{50} = (2.72 \pm 0.20) \mu\text{M}$ ^[d]	n.i.	n.i.
41 (<i>S, rac</i>)					59.1 ± 4.7	n.i.	n.i.	1360 ± 90
41 A (<i>S, R</i>)	3'	4	H	Ph	197 ± 4	n.i.	n.i.	1740 ± 200
41 B (<i>S, S</i>)					n.i.	n.i.	n.i.	1290 ± 50
42 (<i>S, rac</i>)					120 ± 10	n.i.	n.i.	568 ± 36
42 A (<i>S, R</i>)	4'	4	H	Ph	283 ± 14	n.i.	n.i.	1570 ± 150 ^[e]
42 B (<i>S, S</i>)					n.i.	n.i.	n.i.	143 ± 18 ^[e]
43 (<i>R, rac</i>)					58.7 ± 4.6	n.i.	n.i.	359 ± 26
43 A (<i>R, S</i>)	4'	4	H	Ph	n.i.	n.i.	n.i.	166 ± 7
43 B (<i>R, R</i>)					154 ± 20	n.i.	n.i.	1550 ± 70
44 (<i>S, rac</i>)					65.0 ± 2.3	n.i.	n.i.	872 ± 91
44 A (<i>S, R</i>)	4'	4	H	(CH ₂) ₃ NH-Cbz	73.6 ± 5.3	n.i.	n.i.	1450 ± 80
44 B (<i>S, S</i>)					n.i.	n.i.	n.i.	511 ± 65
45 (<i>S, rac</i>)					1750 ± 40	n.i.	n.i.	5900 ± 80
45 A (<i>S, R</i>)	4'	4	SMe	Ph	2790 ± 60	n.i.	n.i.	5370 ± 360 ^[e]
45 B (<i>S, S</i>)					1280 ± 50	n.i.	n.i.	5430 ± 190 ^[e]
46 (<i>S, rac</i>)					n.i.	n.i.	n.i.	n.i.
47 (<i>S, rac</i>)					n.i.	n.i.	n.i.	n.i.

[a] The stereochemistry is given in parentheses. The first entry refers to the configuration at the amino acid, the second to the configuration at the amino-phosphonate. [b] IC_{50} and k_{inac}/K_i values were determined from duplicate measurements with five different inhibitor concentrations. [c] n.i.: no inhibition relates to more than 30% product formation after 30 min at an inhibitor concentration of 30 μM , which corresponds to an IC_{50} value of > 13 μM . Determined from duplicate measurements. [d] No time-dependent inhibition was observed. Rates in the presence of five different inhibitor concentrations, obtained by linear regression of the progress curves, were plotted against inhibitor concentrations to obtain IC_{50} values. [e] The following k_{inac}/K_i values were obtained for inactivation of human trypsin: $(217 \pm 36) \text{M}^{-1} \text{s}^{-1}$ for (*S,R*)-**42 A**, $(65 \pm 13) \text{M}^{-1} \text{s}^{-1}$ for (*S,S*)-**42 B**, $(1480 \pm 214) \text{M}^{-1} \text{s}^{-1}$ for (*S,R*)-**45 A**, and $(1780 \pm 193) \text{M}^{-1} \text{s}^{-1}$ for (*S,S*)-**45 B**.

mined the inactivation of human trypsin by selected compounds (see below). Lower k_{inac}/K_i values were obtained for the human enzyme. Nevertheless, inhibitors **42–45**, and **41**, were not selective for matriptase-2 over trypsin.

Next, we examined the effect of the configuration of the N-terminal amino acid on the inactivator potency toward matriptase-2. Compounds **42** and **43** share the guanidino substitution pattern (*para, para*) and the unsubstituted phenoxy groups (R¹: H), but they differ in the configuration of the phenylalanine moiety. It turned out that the natural *S* configuration caused stronger inhibition of matriptase-2. In the phosphono dipeptide **44**, L-phenylalanine was exchanged for Cbz-protected L-lysine, which reduced the k_{inac}/K_i value (**44** relative to **42**). Thus, L-phenylalanine was maintained as the N-terminal amino acid in the phosphono dipeptides of this study.

At this stage of the chemical optimization, methylthio substituents were introduced into the phenoxy groups of **42**, which resulted in derivative **45**. In accordance with previous reports on the inactivation of other serine proteases by α -aminophosphonates,^[19,26,38] this modification was also favorable for matriptase-2 inhibition and led to a k_{inac}/K_i value of $1750 \text{M}^{-1} \text{s}^{-1}$. In contrast, the replacement of the unsubstituted phenoxy groups in **42** by two ethoxy residues completely abrogated the inhibitory effect of the corresponding compound **46** toward matriptase-2 (Table 1). It is likely that the leaving group abilities of the corresponding P substituents (4-(methylthio)phenoxy > phenoxy > ethoxy) contributed to these differences.

Recently, halogen-containing compounds have been recognized to form noncovalent interactions with Lewis bases. Halogen bonding in protein–ligand interactions is driven by the

anisotropy of electron density on the halogen, which leads to a positively charged region and increases in the order $\text{Cl} < \text{Br} < \text{I}$. Accordingly, by targeting a negatively charged aspartate residue, strong halogen bonding might occur. For non-phosphonate inhibitors of factor Xa, an amidine group could be successfully substituted by iodine.^[44] The bisiodine derivative **47** was included in this study in order to examine whether the same strategy would be applicable to our compounds. However, **47** was inactive (Table 1), which indicated a limited ability for competing with the substrate to interact with the S1 and S3/S4 binding pockets.

In order to elucidate the effect of the configuration at the aminophosphonate carbon atom on the biological activity, the single diastereomers were separated by preparative HPLC and are listed in Table 1. The corresponding code (**A** or **B**) refers to the pattern of NMR resonances as follows. Generally, the **A** diastereomer showed a ¹H NMR signal for the methine POCH proton at higher field and had a larger heteronuclear H–P coupling constant than the corresponding **B** diastereomer. For example, the following signals were obtained for **41 A** and **41 B**: **41 A**: $\delta = 5.93$ ppm (dd, ³*J* (H, H) = 9.8 Hz, ²*J* (H, P) = 22.4 Hz); **41 B**: $\delta = 6.00$ ppm (dd, ³*J* (H, H) = 9.8 Hz, ²*J* (H, P) = 21.8 Hz). The ¹³C NMR signal for the aminophosphonate POCH carbon atom was shifted upfield in the **A** diastereomer relative to the corresponding **B** diastereomer; for example, **41 A**: $\delta = 49.65$ ppm (d, ¹*J* (C, P) = 156.4 Hz); **41 B**: $\delta = 50.03$ ppm (d, ¹*J* (C, P) = 156.4 Hz).

The five pairs of separated epimers clearly differed in their matriptase-2 inhibitory activity. In the cases of **41**, **42**, **44**, and **45**, the **A** diastereomer was the more active one, whereas the corresponding **B** diastereomer showed a weaker activity; for example, $k_{\text{inac}}/K_i = 2790 \text{ M}^{-1} \text{ s}^{-1}$ for **45 A** compared with $1280 \text{ M}^{-1} \text{ s}^{-1}$ for **45 B**. The assignment of the configuration at the phosphonate carbon atom of the active epimer was tentatively achieved by molecular docking. The crystal structures of complexes of serine proteases with phosphonate inactivators revealed that the initially formed serine phosphono diester was converted by hydrolytic “aging” into a phosphono monoester.^[45] The phosphono monoester complexes of matriptase-2 with the two diastereomers of **42** were generated by covalent docking as follows. The single bond between the active-site serine oxygen atom and the phosphorus atom was manually formed and both phenoxy groups were removed from the inhibitor structure. The covalently bound inhibitor was energy minimized within the complex and subjected to covalent docking by using the AutoDock 4.2 program. This procedure yielded a reasonable orientation of the ligand in the case of **42** with an *R*-configured phosphonate carbon atom. Docking indicated that the “Eastern” benzguanidine moiety likely occupied the S1 pocket and formed potential hydrogen bonds to residues Asp756 and Gly787, whereas the “Western” benzguanidine addresses the S3/S4 subsite and is well positioned for hydrogen-bonding interactions to residues Ser664 and Gln741. Moreover, the phenylalanine residue of **42** was likely to form π – π interactions with His617. However, covalent docking with **42** if the phosphonate carbon atom was *S* configured resulted in a less plausible binding mode because of steric constraints

between the active site and the covalently bound inhibitor. Therefore, it is very likely that this epimer of **42** represented the inactive diastereomer and we assigned the (*S,S*) configuration to **42 B**. Accordingly, **42 A** possessed the (*S,R*) configuration. The modeled complex that resulted from the interaction of **42 A** with matriptase-2 and the subsequent hydrolytic “aging” is depicted in Figure 2.

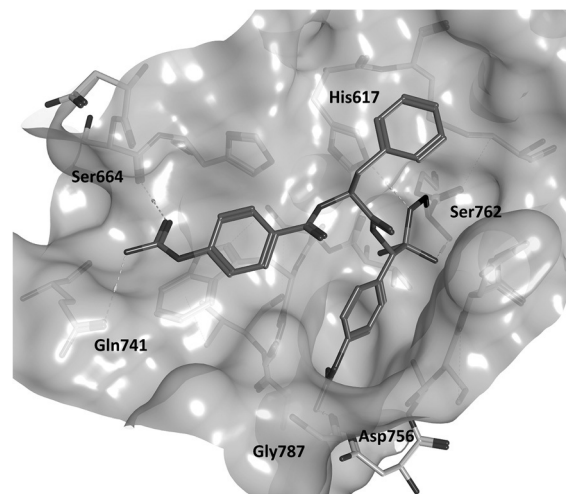


Figure 2. Covalent docking of compound **42 A** (or **45 A**) bound to Ser762 in the binding site of a matriptase-2 homology model. Note that one phenoxy group was removed because of the nucleophilic attack of the active-site serine and formation of the Ser–O–P bond, whereas the other phenoxy group was removed through hydrolysis.

On the basis of this molecular docking approach, the (*S,R*) configuration of the active epimer was concluded to be also valid for **41 A**, **44 A**, and **45 A** (Table 1), whereby **42 A** and **45 A**, which only differ in the aryloxy leaving groups, essentially produce the same phosphono monoester complex with a serine protease. Our findings are in accordance with previous reports on diastereomerically pure phosphonic peptides as serine protease inactivators. First, Boduszek et al. observed a single phosphonate diastereomer to be tenfold more potent at dipeptidyl peptidase IV than the epimeric mixture.^[42] Subsequently, Walker et al. prepared two diphenyl aminophosphonates by asymmetric synthesis and found that the corresponding *R* enantiomer was the stronger inactivator of cathepsin G, chymotrypsin, and human neutrophil elastase.^[46] Winiarski et al. were able to isolate single diastereomers and compared the inhibitory activity towards human neutrophil elastase, porcine pancreatic elastase, chymotrypsin, and trypsin. In all cases, the epimer with an *R*-configured phosphonate warhead was the more potent inactivator.^[38]

In the case of the two epimers of **43** (Table 1), the (*R,R*) configuration was assigned to the active matriptase-2 inhibitor **43 B**. Hence, the *R* configuration at the phosphonate carbon atom permitted a more favorable accommodation of the ligand in the active site, irrespective of the inverted configuration at the amino acid, that is, *R* instead of *S*. The modeled complex of **43 B** and matriptase-2 obtained by covalent dock-

ing is presented in the Supporting Information (Figure S2). Compounds **42A**, **42B**, **43A**, and **43B** represent the four stereoisomers of this structure with **42A** and **43A** forming one and **42B** and **43B** the other enantiomeric pair. As a matter of course, each pair possessed the same NMR signals and, thus, in the case of **43**, the (*R,R*)-configured isomer has to be assigned as **43B**. For the one enantiomeric pair, **42A** was shown to be the more active matriptase-2 inhibitor, that is, the eutomer. For the other pair, **43B** represents the eutomer. The two eutomers displayed a similar binding mode within the active site of matriptase-2, as illustrated by an overlay shown in the Supporting Information (Figure S3). Finally, a comparison of the two eutomers revealed that, if the *R* configuration applies to the phosphonate, the *S* configuration is preferred at the amino acid. Accordingly, **42A** exhibited the strongest inhibition among the four stereoisomers. Introduction of two *para*-methylthio groups into **42A** further improved the activity, and the resultant **45A** turned out to be the most potent matriptase-2 inactivator of the whole series. The kinetic analysis of **45A** is reported in Figure 3.

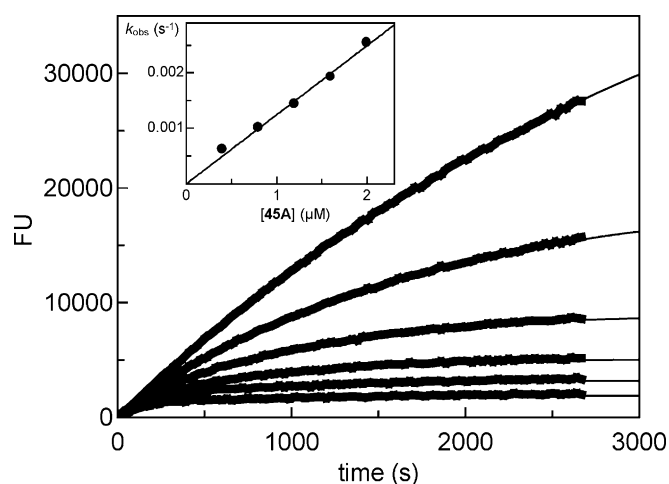


Figure 3. Inhibition of human matriptase-2 by phosphono dipeptide **45A**. From top to bottom: uninhibited reaction, 0.4, 0.8, 1.2, 1.6, and 2 μM . Values of the observed rate constant (k_{obs}) were obtained from nonlinear regression of the progress curves by using the equation $[P] = v_i(1 - e^{-k_{\text{obs}} \times t})/k_{\text{obs}} + d$, in which $[P]$ is the product concentration, v_i is the initial rate, and d is the offset. The inset shows a plot of k_{obs} values (mean of duplicate measurements) versus the inhibitor concentration $[I]$. Linear regression gave a $k_{\text{obs}}/[I]$ value of $(1240 \pm 30) \text{ M}^{-1} \text{ s}^{-1}$.

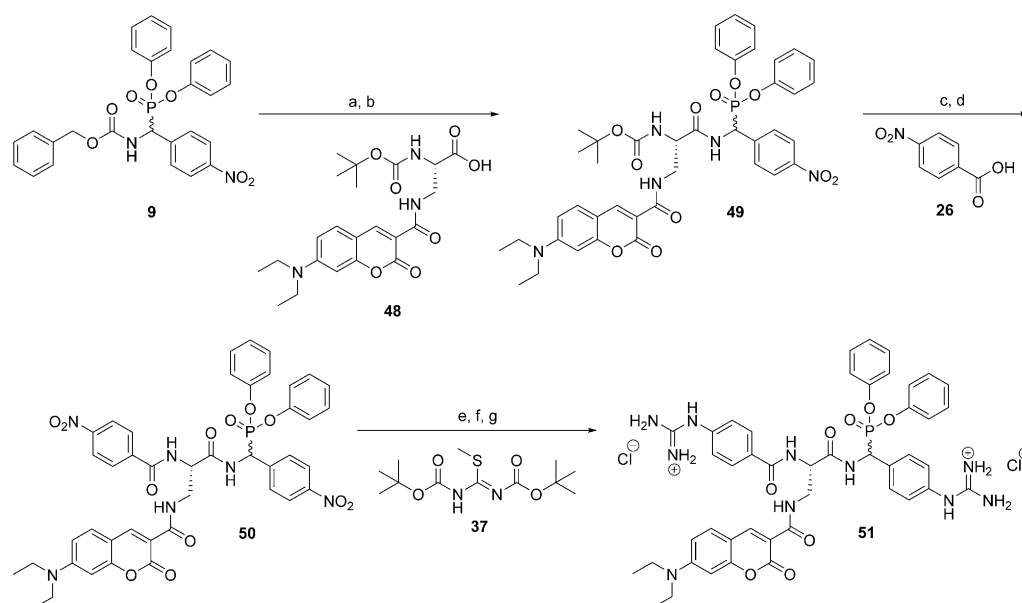
Whereas the cell-free enzyme assays for matriptase-2 were performed with the conditioned medium of transfected human embryonic kidney (HEK) cells as the enzyme source,^[7,11,29] inactivator **45A** was chosen for a further study with intact cells. Matriptase-2 is a membrane-bound protease with an extracellular catalytic domain, so inhibition of the cell-surface-associated enzymatic activity was investigated. For this purpose, adherent, transfected HEK cells in a 96-well plate were washed and treated with **45A** and the consumption of the peptidic substrate was monitored. Actually, treatment with 750 nM **45A** led to an instantaneous and nearly complete in-

activation of matriptase-2, as shown in Figure S4 in the Supporting Information.

The efficient inactivation of matriptase-2 by phosphono bisbenzguanidines prompted us to design a first activity-based probe for matriptase-2 by utilizing this chemotype. Two of the three required elements of an activity-based probe have already been assembled in the structures of inactivators **41–45**, that is, the phosphonate warhead and the benzguanidine recognition elements. It was intended to introduce the fluorescent reporter tag as part of the central amino acid. Thus, a fluorescent amino acid of rather small size and with physicochemical properties similar to those of phenylalanine was chosen. Coumarins with donor groups at position 7 represent a widely used class of fluorescent dyes. Their small molecular size, high fluorescence quantum yields, and large Stokes shifts, as well as chemical and enzymatic stability, are favored properties.^[41,47–49]

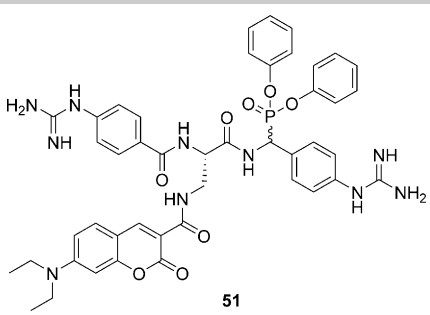
Thus, for the generation of the activity-based probe **51** (Scheme 2), we employed the coumarin-labeled amino acid **48**.^[47] Attempts to incorporate **48** into a bis(4-(methylthio)phenylphosphono) bisbenzguanidine failed. However, we succeeded in preparing the final compound **51**, a structural analogue of inactivator **42**. The final steps in the preparation of **51** were essentially the same as those described for the nonlabeled phosphono bisbenzguanidines. Compound **51** contains two benzguanidine moieties to interact with the S1 and S3/S4 specificity pockets, the phosphonate warhead for an irreversible attachment of the probe to the target, an appropriate coumarin as a fluorescent label, and the central amino acid in the preferred *S* configuration. As executed for the other diastereomers, the racemic compound **51** was separated into the two epimers, designated as **51A** and **51B**. In Table 2, the kinetic parameters of **51**, **51A**, and **51B** are outlined, which revealed again inhibitory activity for the *R*-configured phosphonate (**51A**), whereas the epimer possessing the *S*-configured phosphonate (**51B**) was inactive toward matriptase-2.

The applicability of **51A** as an activity-based probe for matriptase-2 was demonstrated by using the conditioned medium of stably transfected HEK cells as a source of matriptase-2, which was tagged with the c-Myc peptide and polyhistidine (His6). The conditioned medium was collected and concentrated, then different amounts (20–100 μg of total protein) were incubated with 100 μM compound **51A** for 30 min and subjected to sodium dodecylsulfate polyacrylamide-gel electrophoresis (SDS-PAGE). A fluorescent band at 30 kDa was clearly visible in samples containing matriptase-2 (Figure 4A, lanes 1–5). This demonstrated the sensitivity of the probe to detect the amount of matriptase-2 that is present in 20 μg of total protein. A detection limit for matriptase-2 could not be determined because of the lack of sufficiently purified enzyme. The specificity of the probe for matriptase-2 was verified with HEK mock cells as a negative control; these cells were carrying the empty vector and expressing no endogenous matriptase-2.^[2] The conditioned medium of HEK mock cells (100 μg of total protein) was treated likewise with **51A** and no fluorescent band was visible at 30 kDa (Figure 4A, lane 6), which provided evidence of labeled matriptase-2 in lanes 1–5. The protein patterns of the conditioned media were visualized by Coomassie



Scheme 2. Synthesis of the activity-based probe **51**. Reaction conditions: a) AcOH/HBr, RT; b) HATU, DIPEA, DMF, RT; c) TFA, CH₂Cl₂, RT; d) HATU, DIPEA, DMF, RT; e) SnCl₂·2H₂O, H₂O, EtOAc, reflux; f) HgCl₂, TEA, CH₂Cl₂, RT; g) TFA, CH₂Cl₂, RT, prep. HPLC, HCl, lyophilization.

Table 2. Inhibition of matriptase-2 by the activity-based probes of type **51**.



Comp. ^[a]	Enzyme inactivation, k_{inac}/K_i [$\text{M}^{-1} \text{s}^{-1}$] ^[b,c]			
	Human matriptase-2	Human thrombin	Bovine factor Xa	Bovine trypsin
51 (<i>S, rac</i>)	34.5 ± 0.7	IC ₅₀ = (21.5 ± 2.2) μM ^[d]	n.i.	108 ± 8
51 A (<i>S, R</i>)	50.4 ± 0.6	IC ₅₀ = (45.8 ± 5.6) μM ^[d]	n.i.	148 ± 10 ^[e]
51 B (<i>S, S</i>)	n.i.	IC ₅₀ = (15.5 ± 1.7) μM ^[d]	n.i.	92.2 ± 12.1 ^[e]

[a] The stereochemistry is given in parentheses. The first entry refers to the configuration at the amino acid, the second to the configuration at the aminophosphonate. [b] IC₅₀ and k_{inac}/K_i values were determined from duplicate measurements with five different inhibitor concentrations. [c] n.i.: no inhibition relates to less than 30% product formation after 30 min at an inhibitor concentration of 30 μM, which corresponds to an IC₅₀ value of > 13 μM. Determined from duplicate measurements. [d] No time-dependent inhibition was observed. Rates in the presence of five different inhibitor concentrations, obtained by linear regression of the progress curves, were plotted against inhibitor concentrations to obtain IC₅₀ values. [e] The following k_{inac}/K_i values were obtained for inactivation of human trypsin: (81.5 ± 14.6) M⁻¹s⁻¹ for (*S, R*)-**51 A** and (58.7 ± 11.6) M⁻¹s⁻¹ for (*S, S*)-**51 B**.

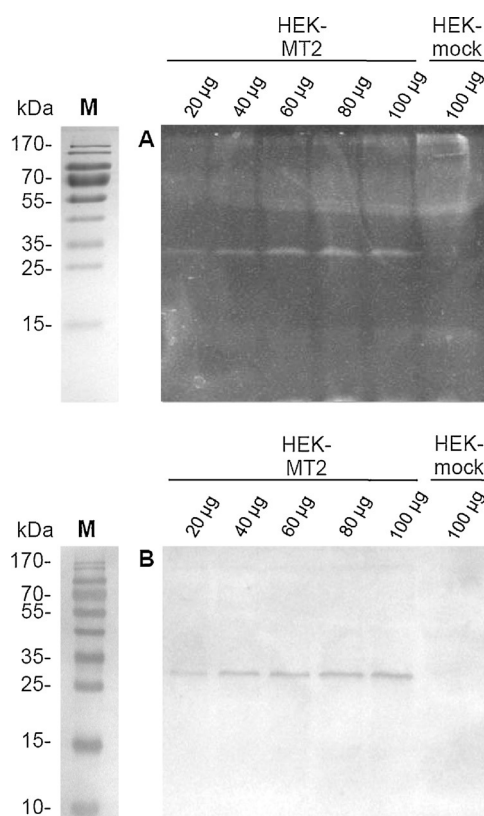


Figure 4. Imaging of human matriptase-2 with the fluorescent probe **51 A**. Different amounts of conditioned medium of transfected HEK cells expressing matriptase-2 (HEK-MT2; total protein amounts of 20 μg/18 μL to 100 μg/18 μL) were incubated with 100 μM **51 A**. In a control experiment, a conditioned medium of HEK mock cells (100 μg/18 μL) was treated with 100 μM **51 A**. Labeling reactions were performed for 30 min at 37 °C. The proteins were separated by SDS-PAGE and visualized by A) fluorescence detection. B) The untreated conditioned medium was analyzed by western blotting with a monoclonal mouse anti-c-Myc antibody. M: molecular mass marker.

brilliant blue staining (Figure S5C in the Supporting Information), which indicated sufficiently selective labeling of the target matriptase-2 in the presence of a large excess of other proteins. The indistinct signal visualized by fluorescence detection in the range of 40–170 kDa (Figure 4A) resulted from unspecific interaction of the probe with the proteins present in high concentrations that originate from the medium used for cell culturing and from the HEK cells (see Figure S5C and S5D in the Supporting Information).

As a positive control to prove the identity of matriptase-2, the conditioned media of HEK cells expressing matriptase-2 and HEK mock cells were analyzed by SDS-PAGE, without treatment with **51 A** (Figure 4B; corresponding Ponceau S staining in Figure S5D in the Supporting Information) and matriptase-2 was visualized by western blot analysis by using a monoclonal mouse anti-c-Myc antibody (Figure 4B, lanes 1–5). Notably, the sensitivity of the activity-based probe **51 A** to label matriptase-2 was comparable to the reliably efficient immunodetection of the Myc tag. Although western blotting addresses the total amount of the target, activity-based probes such as **51 A** lead to selective labeling of only the catalytically active form.

Conclusion

We discovered phosphono bisbenzguanidines as dipeptidomimetic inactivators for matriptase-2. The design was based on the twofold introduction of benzguanidine moieties to occupy the S1 and S3/S4 binding sites, respectively. Furthermore, a phosphonate warhead was introduced to facilitate the covalent linkage to the active-site serine. Nine compounds (**39–47**) comprising this series were synthesized and evaluated toward the serine proteases matriptase-2, human thrombin, bovine factor Xa, and trypsin. Structural optimization and structure–activity relationship analyses led to the development of compound **45** with a k_{inac}/K_i value of $1750 \text{ M}^{-1} \text{ s}^{-1}$ towards matriptase-2. Each product was obtained as a mixture of two diastereomers and the biologically active products were separated into their single epimers. The inhibitors with *R* configuration at the phosphonate carbon atom were found to be more potent than the corresponding *S* epimers. The *R*-configured **45A** possessed a k_{inac}/K_i value of $2790 \text{ M}^{-1} \text{ s}^{-1}$ and represents the most potent irreversible inhibitor of matriptase-2 known so far. This phosphono bisbenzguanidine might serve as a starting point for further structure modifications of matriptase-2 inactivators. To verify the suitability of **45A**, we demonstrated for the first time that the activity of membrane-bound matriptase-2 of adherent, intact cells was abolished upon treatment with a low-molecular-weight inhibitor. By applying the chemotype of phosphono bisbenzguanidines, we successfully employed the activity-based probe **51 A** for direct in-gel fluorescence detection of matriptase-2 in a complex protein mixture. The phosphono bisbenzguanidine inactivators are expected to serve as valuable tool compounds for future investigations of the key role of matriptase-2 in iron homeostasis. In particular, **45A** might be useful to block matriptase-2 activity in control experiments in the development of activity-based probes of other chemotypes targeting matriptase-2.

Experimental Section

Preparation of phosphono bisbenzguanidines **45 A** and **45 B**

Benzyl (bis(4-(methylthio)phenoxy)phosphoryl)(4-nitrophenyl)methylcarbamate (10): 4-(Methylthio)phenol (**2**; 4.2 g, 30.0 mmol) was added to a flask containing phosphorus trichloride (1.37 g, 0.87 mL, 10.0 mmol) dissolved in acetonitrile (40 mL). The mixture was heated under reflux for 3 h. The solvent was removed in vacuo and the crude product, the triarylphosphite **3**, was used directly for the amidoalkylation reaction. 4-Nitrobenzaldehyde (**6**; 1.51 g, 10.0 mmol), benzyl carbamate (**4**; 1.51 g, 10.0 mmol), and phosphite **3** were combined with glacial acetic acid (50 mL). The solution was stirred at 90 °C for 3 h. The acetic acid was removed in vacuo and the crude product was dissolved in MeOH (100 mL). The solution was kept at 4 °C overnight until the precipitation of the protected α -aminophosphonate was complete. Compound **10** was obtained by filtration and drying as a white solid (3.66 g, 60%); m.p. 147–150 °C (lit. [19]: m.p. 135 °C); $^1\text{H NMR}$ (500 MHz, $[\text{D}_6]\text{DMSO}$, 30 °C): δ = 2.42 (s, 3H), 2.43 (s, 3H), 5.06 (d, 2J = 12.3 Hz, 1H), 5.14 (d, 2J = 12.3 Hz, 1H), 5.83 (dd, 3J = 10.1 Hz, 2J = 23.6 Hz, 1H), 6.97 (d, 3J = 8.2 Hz, 2H), 7.02 (d, 3J = 7.9 Hz, 2H), 7.21–7.23 (m, 4H), 7.29–7.39 (m, 5H), 7.91 (dd, 4J = 1.9 Hz, 3J = 8.8 Hz, 2H), 8.25 (d, 3J = 8.5 Hz, 2H), 9.04 ppm (d, 3J = 9.8 Hz, 1H); $^{13}\text{C NMR}$ (125 MHz, $[\text{D}_6]\text{DMSO}$, 30 °C): δ = 15.38, 15.41, 52.63 (d, J = 154.2 Hz), 66.53, 120.93 (d, J = 4.0 Hz), 121.02 (d, J = 3.7 Hz), 123.65, 127.71, 127.75, 128.14, 128.50, 129.79, 129.83, 135.04, 135.18, 136.62, 142.12, 147.28 (d, J = 9.7 Hz), 147.48, 147.51, 147.61 (d, J = 9.7 Hz), 156.08 ppm (d, J = 8.4 Hz); LC-MS (ESI): purity 98%, m/z 611.16 $[\text{M}+\text{H}]^+$, 608.90 $[\text{M}-\text{H}]^-$; elemental analysis: calcd for $\text{C}_{29}\text{H}_{27}\text{N}_2\text{O}_7\text{PS}_2$: C 57.04, H 4.46, N 4.59; found: C 57.02, H 4.45, N 4.78.

(S)-tert-Butyl 1-((bis(4-(methylthio)phenoxy)phosphoryl)(4-nitrophenyl)methylamino)-1-oxo-3-phenylpropan-2-ylcarbamate (21): The protected α -aminophosphonate **10** (0.696 g, 1.14 mmol) was dissolved in a solution of HBr (33%) in acetic acid (20 mL) and stirred for 30 min at room temperature. The solvent was removed in vacuo and the crude product **13** was obtained after precipitation in ethyl acetate (50 mL). Boc-L-Phe-OH (**14**; 0.302 g, 1.14 mmol) was dissolved in anhydrous DMF (20 mL) and activated for 15 min at room temperature with HATU (0.433 g, 1.14 mmol) and DIPEA (0.439 g, 3.42 mmol). Afterwards, amine **13** (0.635 g, 1.14 mmol) was added and the mixture was stirred overnight at room temperature.^[35] Product **21** was purified by column chromatography on silica gel with petroleum ether:ethyl acetate (3:1) as the eluent to obtain a white solid (0.512 g, 62%); m.p. 89–92 °C; $^1\text{H NMR}$ (500 MHz, $[\text{D}_6]\text{DMSO}$, 30 °C, mixture of diastereomers, ratio of approximately 1:1 according to $^1\text{H NMR}$ spectroscopy): δ = 1.25 (s, 9H), 1.31 (s, 9H), 2.40 (s, 3H), 2.41–2.42 (m, 9H), 2.68–2.76 (m, 2H), 2.81–2.91 (m, 2H), 4.40–4.47 (m, 1H), 4.49–4.56 (m, 1H), 6.02 (dd, 3J = 9.5 Hz, 2J = 23.0 Hz, 1H), 6.11 (dd, 3J = 9.6 Hz, 2J = 23.2 Hz, 1H), 6.95 (d, 3J = 8.5 Hz, 2H), 6.98–7.07 (m, 8H), 7.16–7.30 (m, 18H), 7.77 (d, 3J = 7.3 Hz, 2H), 7.92 (d, 3J = 7.3 Hz, 2H), 8.22 (d, 3J = 8.9 Hz, 2H), 8.29 (d, 3J = 8.9 Hz, 2H), 9.38 (d, 3J = 10.1 Hz, 1H), 9.63 ppm (dd, 4J = 2.7 Hz, 3J = 9.6 Hz, 1H); $^{13}\text{C NMR}$ (125 MHz, $[\text{D}_6]\text{DMSO}$, 30 °C, mixture of diastereomers, ratio of approximately 1:1 according to $^1\text{H NMR}$ spectroscopy): δ = 15.34, 15.38, 28.21, 28.27, 37.26, 37.47, 49.68 (d, J = 155.6 Hz), 50.05 (d, J = 153.9 Hz), 55.57, 55.62, 78.26, 78.28, 121.00, 121.16 (d, J = 3.5 Hz), 121.43 (d, J = 3.2 Hz), 123.69, 126.34, 126.41, 127.71, 127.75, 128.01, 128.16, 129.26, 129.40, 129.63, 129.67, 129.80, 129.84, 135.22, 135.28, 137.73, 137.93, 141.92, 142.15, 147.19–147.51 (m), 155.43, 155.54, 172.30–172.45 ppm (m); LC-MS (ESI): purity 95%, m/z 741.37 $[\text{M}+\text{NH}_4]^+$; el-

emental analysis: calcd for $C_{35}H_{38}N_3O_8PS_2$: C 58.08, H 5.29, N 5.81; found: C 58.16, H 5.66, N 5.67.

(S)-Bis(4-(methylthio)phenyl) (2-(4-nitrobenzamido)-3-phenylpropanamido)(4-nitrophenyl)methylphosphonate (34): The N-protected phosphonate **21** (2.512 g, 3.47 mmol) was dissolved in a solution of dichloromethane and trifluoroacetic acid (1:1, 20 mL) and stirred for 1 h at room temperature. Product **24** was obtained after removal of the solvent in vacuo. 4-Nitrobenzoic acid (**26**; 0.580 g, 3.47 mmol) was dissolved in anhydrous DMF (20 mL) and activated for 15 min at room temperature with HATU (1.319 g, 3.47 mmol) and DIPEA (1.345 g, 10.41 mmol). Afterwards, amine **24** (2.560 g, 3.47 mmol) was added and the mixture was stirred overnight at room temperature.^[35] A volume of 1 mL of *n*-heptane was added to the solution and a white precipitate was formed. The pure product **34** was obtained by suction filtration (1.180 g, 44%); m.p. 191–193 °C; ¹H NMR (500 MHz, [D₆]DMSO, 30 °C, mixture of diastereomers, ratio of approximately 7:1 (A:B) according to ¹H NMR spectroscopy): δ = 2.38 (s, 3H), 2.39 (s, 3H), 2.40 (s, 3H), 2.42 (s, 3H), 2.91–3.05 (m, 4H), 4.97–5.02 (m, 1H), 5.11–5.17 (m, 1H), 6.06 (dd, ³J = 9.6 Hz, ²J = 23.2 Hz, 1H), 6.16 (dd, ³J = 9.8 Hz, ²J = 22.7 Hz, 1H), 6.99 (t, ³J = 8.0 Hz, 4H), 7.07 (d, ³J = 7.9 Hz, 2H), 7.10–7.28 (m, 7H), 7.34 (d, ³J = 7.0 Hz, 2H), 7.37 (d, ³J = 7.0 Hz, 2H), 7.83 (dd, ⁴J = 1.9 Hz, ³J = 8.8 Hz, 2H), 7.93–7.96 (m, 4H), 8.03 (d, ³J = 9.1 Hz, 2H), 8.24 (d, ³J = 8.8 Hz, 2H), 8.27–8.32 (m, 2H), 9.02 (d, ³J = 8.6 Hz, 1H), 9.11 (d, ³J = 8.6 Hz, 1H), 9.69 (dd, ⁴J = 2.4 Hz, ³J = 9.6 Hz, 1H), 9.89 ppm (dd, ⁴J = 2.9 Hz, ³J = 9.5 Hz, 1H); ¹³C NMR (125 MHz, [D₆]DMSO, 30 °C, mixture of diastereomers, ratio of approximately 7:1 (A:B) according to ¹H NMR spectroscopy): δ = 15.33, 15.38, 37.06, 37.28, 49.87 (d, *J* = 154.4 Hz), 54.77, 55.01, 121.01 (d, *J* = 4.0 Hz), 121.28 (d, *J* = 3.5 Hz), 123.62, 123.73, 126.51, 126.58, 127.67, 127.70, 127.78, 128.14, 128.28, 129.00, 129.08, 129.22, 129.37, 129.70, 129.74, 129.95, 129.89, 135.24, 137.64, 137.94, 139.50, 139.57, 141.80, 141.92, 147.16–147.44 (m), 149.28, 164.98, 164.90, 171.66 ppm (d, *J* = 7.7 Hz); the following C atoms of the **B** diastereomer were not detectable: POCH, CONHCP, and the C1 carbon atoms of both phenoxy groups; LC-MS (ESI): purity 97%, *m/z* 773.3 [M+H]⁺; elemental analysis: calcd for $C_{37}H_{33}N_4O_9PS_2$: C 57.51, H 4.30, N 7.25; found: C 57.37, H 4.52, N 7.25.

(S)-Bis(4-(methylthio)phenyl) (2-(4-guanidinobenzamido)-3-phenylpropanamido)(4-guanidinophenyl)methylphosphonate dihydrochloride (45): SnCl₂·2H₂O (3.09 g, 13.7 mmol) and H₂O (0.99 g, 54.8 mmol) were added to a stirred solution of **34** (1.061 g, 1.37 mmol) in EtOAc (40 mL). The solution was stirred under reflux for 4 h. The solvent was removed in vacuo and the residue was suspended in 2 N NaOH (100 mL). The mixture was extracted with dichloromethane (3 × 100 mL). The combined organic extracts were washed with H₂O (100 mL) and brine (100 mL). The material was dried over Na₂SO₄ and evaporated to obtain the corresponding amino phosphonate intermediate **36**, which was purified by column chromatography with ethyl acetate. The amino phosphonate **36** (0.600 g, 0.84 mmol) was treated with *N,N'*-di-Boc-*S*-methylisothiourea (**37**; 0.439 g, 1.51 mmol), HgCl₂ (0.433 g, 1.60 mmol), and Et₃N (0.255 g, 2.52 mmol) in dichloromethane (20 mL) at room temperature for 24 h. The solution was passed through a pad of Celite and washed with dichloromethane (50 mL) and methanol (50 mL). The solvents were removed in vacuo. The resulting Boc-protected guanidine **38** was purified by column chromatography, with ethyl acetate:petroleum ether:TEA (1:1:0.002). Compound **38** was dissolved in dichloromethane (5 mL) and a 50% solution of trifluoroacetic acid in dichloromethane (10 mL) was added. After being stirred at room temperature for 2 h, the solvent was evaporated. The resulting oil was purified by preparative HPLC. The HPLC method was as follows: MeOH:H₂O (40:60), 17 min. A few drops of

1 N HCl were added to the product to form the hydrochloride salt. The final products **45A** and **45B** were obtained as white solids after lyophilization (92 mg **A** and 7 mg **B**, 8% over three steps).

Diastereomer 45A with (COCH-S, POCH-R) configuration: M.p. 169–172 °C; ¹H NMR (500 MHz, [D₆]DMSO, 30 °C): δ = 2.40 (s, 3H), 2.41 (s, 3H), 2.97–2.99 (m, 2H), 5.10 (q, ³J = 8.7 Hz, 1H), 5.90 (dd, ³J = 9.8 Hz, ²J = 22.4 Hz, 1H), 6.99 (d, ³J = 8.2 Hz, 2H), 7.00 (d, ³J = 8.2 Hz, 2H), 7.26–7.24 (m, 7H), 7.27 (t, ³J = 8.2 Hz, 4H), 7.38 (d, ³J = 7.3 Hz, 2H), 7.56 (s, 4H), 7.64–7.66 (m, 6H), 7.92 (d, ³J = 8.6 Hz, 2H), 8.78 (d, ³J = 8.5 Hz, 1H), 9.78 (d, ³J = 7.9 Hz, 1H), 10.08 ppm (brs, 2H); ¹³C NMR (125 MHz, [D₆]DMSO, 30 °C): δ = 15.42, 15.43, 37.32, 49.55 (d, *J* = 156.1 Hz), 54.82, 121.20 (d, *J* = 3.7 Hz), 121.41 (d, *J* = 3.5 Hz), 123.12, 123.94, 126.45, 127.71, 128.13, 129.13, 129.41, 129.77, 129.81, 131.12, 132.09, 135.04, 135.57, 135.59, 138.08, 138.59, 147.38 (d, *J* = 10.2 Hz), 147.48 (d, *J* = 10.4 Hz), 155.98, 156.01, 165.52, 171.92 (d, *J* = 7.2 Hz); LC-MS (ESI): purity 97%, *m/z* 797.4 [M+H]⁺; HRMS (ESI⁺): *m/z* calcd for $C_{39}H_{41}N_8O_5PS_2$ [M+H]⁺: 797.2452; found: 797.2452.

Diastereomer 45B with (COCH-S, POCH-S) configuration: M.p. 167–170 °C; ¹H NMR (500 MHz, [D₆]DMSO, 30 °C): δ = 2.40 (s, 3H), 2.42 (s, 3H), 2.95 (d, ³J = 6.6 Hz, 2H), 5.13 (q, ³J = 6.6 Hz, 1H), 5.90 (dd, ³J = 8.1 Hz, ²J = 18.5 Hz, 1H), 6.98 (d, ³J = 7.1 Hz, 2H), 6.99 (d, ³J = 6.9 Hz, 2H), 7.14 (t, ³J = 6.2 Hz, 1H), 7.18 (d, ³J = 7.4 Hz, 2H), 7.19 (d, ³J = 7.2 Hz, 2H), 7.22 (t, ³J = 6.3 Hz, 2H), 7.27 (d, ³J = 6.9 Hz, 4H), 7.38 (d, ³J = 6.1 Hz, 2H), 7.41 (s, 4H), 7.43–7.50 (m, 4H), 7.65 (dd, ⁴J = 1.2 Hz, ³J = 7.1 Hz, 2H), 7.90 (d, ³J = 7.1 Hz, 2H), 8.71 (d, ³J = 7.1 Hz, 1H), 9.78 (d, ³J = 8.6 Hz, 1H), 9.63–9.92 ppm (brs, 2H); ¹³C NMR (125 MHz, [D₆]DMSO, 30 °C): δ = 15.38, 15.39, 121.14 (d, *J* = 4.5 Hz), 121.40 (d, *J* = 3.5 Hz), 123.37, 124.16, 127.68, 128.10, 129.10, 129.36, 129.73, 129.77, 132.19, 135.05, 155.65, 155.69, 164.79 ppm; the following C atoms were not detectable: CONHCH₂, COCH, POCH, CONHCP, and the C1 carbon atoms of both phenoxy groups; LC-MS (ESI): purity 94%, *m/z* 797.2 [M+H]⁺; HRMS (ESI⁺): *m/z* calcd for $C_{39}H_{41}N_8O_5PS_2$ [M+H]⁺: 797.2452; found: 797.2455.

Acknowledgements

D.H. holds a fellowship from the Bonn International Graduate School of Drug Sciences (BIGS DrugS). D.H. was also supported by a fellowship from the NRW International Graduate Research School Biotech-Pharma, and N.F. by a fellowship from the Jürgen Manchot Foundation, Düsseldorf, Germany. M.S. and M.M. are supported by the Maria von Linden program of the University of Bonn. M.S. is also supported by the German Research Foundation (STI 660/1-1). The authors thank Tamara Scheidt for assistance.

Keywords: enzymes • fluorescent probes • inhibitors • peptidomimetics • serine proteases

- [1] T. H. Bugge, T. M. Antalis, Q. Wu, *J. Biol. Chem.* **2009**, *284*, 23177–23181.
- [2] G. Velasco, S. Cal, V. Quesada, L. M. Sánchez, C. López-Otín, *J. Biol. Chem.* **2002**, *277*, 37637–37646.
- [3] a) K. E. Finberg, M. M. Heeney, D. R. Campagna, Y. Aydinok, H. A. Pearson, K. R. Hartman, M. M. Mayo, S. M. Samuel, J. J. Strouse, K. Markianos, N. C. Andrews, M. D. Fleming, *Nat. Genet.* **2008**, *40*, 569–571; b) X. Du, E. She, T. Gelbart, J. Truksa, P. Lee, Y. Xia, K. Khovananth, S. Mudd, N. Mann, E. M. Moresco, E. Beutler, B. Beutler, *Science* **2008**, *320*, 1088–1092; c) A. R. Folgueras, F. M. de Lara, A. M. Pendás, C. Garabaya, F. Rodríguez, A. Astudillo, T. Bernal, R. Cabanillas, C. López-Otín, G. Velasco, *Blood* **2008**, *112*, 2539–2645.

- [4] a) K. Finberg, *J. Clin. Invest.* **2013**, *123*, 1424–1427; b) M. Stirnberg, M. Gütschow, *Curr. Pharm. Des.* **2013**, *19*, 1052–1061; c) C. Y. Wang, D. Meynard, H. Y. Lin, *Front. Pharmacol.* **2014**, *5*, 114; d) C. J. McDonald, L. Ostini, N. Bennett, N. Subramaniam, J. Hooper, G. Velasco, D. F. Wallace, V. N. Subramaniam, *Am. J. Physiol. Cell Physiol.* **2015**, *308*, C539–C547.
- [5] L. Silvestri, A. Pagani, A. Nai, I. De Domenico, J. Kaplan, C. Camaschella, *Cell Metab.* **2008**, *8*, 502–511.
- [6] a) J. E. Maxson, J. Chen, C. A. Enns, A. S. Zhang, *J. Biol. Chem.* **2010**, *285*, 39021–39028; b) M. Rausa, M. Ghitti, A. Pagani, A. Nai, A. Campanella, G. Musco, C. Camaschella, L. Silvestri, *J. Cell. Mol. Med.* **2015**, *19*, 879–888.
- [7] M. Stirnberg, E. Maurer, A. Horstmeyer, S. Kolp, S. Frank, T. Bald, K. Arenz, A. Janzer, K. Prager, P. Wunderlich, J. Walter, M. Gütschow, *Biochem. J.* **2010**, *430*, 87–95.
- [8] F. Bélièveau, A. Désilets, R. Leduc, *FEBS J.* **2009**, *276*, 2213–2226.
- [9] M. Wysocka, N. Gruba, A. Miecznikowska, J. Popow-Stellmaszyk, M. Gütschow, M. Stirnberg, N. Furtmann, J. Bajorath, A. Lesner, K. Rolka, *Biochimie* **2014**, *97*, 121–127.
- [10] L. De Falco, M. Sanchez, L. Silvestri, C. Kannengiesser, M. U. Muckenthaler, A. Iolascon, L. Gouya, C. Camaschella, C. Beaumont, *Haematologica* **2013**, *98*, 845–853.
- [11] M. T. Sisay, T. Steinmetzer, M. Stirnberg, E. Maurer, M. Hammami, J. Bajorath, M. Gütschow, *J. Med. Chem.* **2010**, *53*, 5523–5535.
- [12] a) Y. Ginzburg, S. Rivella, *Blood* **2011**, *118*, 4321–4330; b) P. J. Schmidt, M. D. Fleming, *Hematol. Oncol. Clin. North Am.* **2014**, *28*, 387–401.
- [13] P. J. Schmidt, I. Toudjarska, A. K. Sendamarai, T. Racie, S. Milstein, B. R. Bettencourt, J. Hettinger, D. Bumcrot, M. D. Fleming, *Blood* **2013**, *121*, 1200–1208.
- [14] S. Guo, C. Casu, S. Gardenghi, S. Booten, M. Aghajan, R. Peralta, A. Watt, S. Freier, B. P. Monia, S. Rivella, *J. Clin. Invest.* **2013**, *123*, 1531–1541.
- [15] M. Sieńczyk, J. Oleksyszyn, *Curr. Med. Chem.* **2009**, *16*, 1673–1687.
- [16] a) M. H. Potashman, M. E. Duggan, *J. Med. Chem.* **2009**, *52*, 1231–1246; b) D. S. Johnson, E. Weerapana, B. F. Cravatt, *Future Med. Chem.* **2010**, *2*, 949–964; c) J. Singh, R. C. Petter, T. A. Baillie, A. Whitty, *Nat. Rev. Drug Discovery* **2011**, *10*, 307–317.
- [17] R. A. Bauer, *Drug Discovery Today* **2015**, *20*, 1061–1073.
- [18] J. Oleksyszyn, B. Boduszek, C. M. Kam, J. C. Powers, *J. Med. Chem.* **1994**, *37*, 226–231.
- [19] M. Sieńczyk, J. Oleksyszyn, *Bioorg. Med. Chem. Lett.* **2006**, *16*, 2886–2890.
- [20] S. Serim, S. V. Mayer, S. H. Verhelst, *Org. Biomol. Chem.* **2013**, *11*, 5714–5721.
- [21] S. Serim, P. Baer, S. H. G. Verhelst, *Org. Biomol. Chem.* **2015**, *13*, 2293–2299.
- [22] a) D. S. Jackson, S. A. Fraser, L. M. Ni, C. M. Kam, U. Winkler, D. A. Johnson, C. J. Froelich, D. Hudig, J. C. Powers, *J. Med. Chem.* **1998**, *41*, 2289–2301; b) C. M. Brown, M. Ray, A. A. Eroy-Reveles, P. Egea, C. Tajon, C. S. Craik, *Chem. Biol.* **2011**, *18*, 48–57.
- [23] J. Joossens, O. M. Ali, I. El-Sayed, G. Surpateanu, P. Van der Veken, A. M. Lambeir, B. Setyono-Han, J. A. Foekens, A. Schneider, W. Schmalix, A. Haemers, K. Augustyns, *J. Med. Chem.* **2007**, *50*, 6638–6646.
- [24] a) J. Joossens, P. Van der Veken, A. M. Lambeir, K. Augustyns, A. Haemers, *J. Med. Chem.* **2004**, *47*, 2411–2413; b) J. Joossens, P. Van der Veken, G. Surpateanu, A. M. Lambeir, I. El-Sayed, O. M. Ali, K. Augustyns, A. Haemers, *J. Med. Chem.* **2006**, *49*, 5785–5793.
- [25] L. M. Ni, J. C. Powers, *Bioorg. Med. Chem.* **1998**, *6*, 1767–1773.
- [26] M. Sieńczyk, A. Lesner, M. Wysocka, A. Legowska, E. Pietrusewicz, K. Rolka, J. Oleksyszyn, *Bioorg. Med. Chem.* **2008**, *16*, 8863–8867.
- [27] a) W. D. Wilson, F. A. Tanius, A. Mathis, D. Tevis, J. E. Hall, D. W. Boykin, *Biochimie* **2008**, *90*, 999–1014; b) T. L. Huang, A. Mayence, J. J. Van den Eynde, *Bioorg. Med. Chem.* **2014**, *22*, 1983–1992.
- [28] a) O. Vázquez, M. I. Sánchez, J. Martínez-Costas, M. E. Vázquez, J. L. Mascareñas, *Org. Lett.* **2010**, *12*, 216–219; b) M. I. Sánchez, O. Vázquez, M. E. Vázquez, J. L. Mascareñas, *Chem. Eur. J.* **2013**, *19*, 9923–9929.
- [29] S. Dosa, M. Stirnberg, V. Lülldorff, D. Häußler, E. Maurer, M. Gütschow, *Bioorg. Med. Chem.* **2012**, *20*, 6489–6505.
- [30] E. Maurer, M. T. Sisay, M. Stirnberg, T. Steinmetzer, J. Bajorath, M. Gütschow, *ChemMedChem* **2012**, *7*, 68–72.
- [31] M. Hammami, E. Rühmann, E. Maurer, A. Heine, M. Gütschow, G. Klebe, T. Steinmetzer, *Med. Chem. Commun.* **2012**, *3*, 807–813.
- [32] D. Duchêne, E. Colombo, A. Désilets, P. L. Boudreault, R. Leduc, E. Marsault, R. Najmanovich, *J. Med. Chem.* **2014**, *57*, 10198–10204.
- [33] a) E. Sabidó, T. Tarragó, S. Niessen, B. F. Cravatt, E. Giralt, *ChemBioChem* **2009**, *10*, 2361–2366; b) P. M. Mumford, G. J. Tarver, M. Shipman, *J. Org. Chem.* **2009**, *74*, 3573–3575; c) E. Sabidó, T. Tarragó, E. Giralt, *Bioorg. Med. Chem.* **2010**, *18*, 8350–8355.
- [34] a) A. B. Berger, P. M. Vitorino, M. Bogoy, *Am. J. Pharmacogenomics* **2004**, *4*, 371–381; b) M. Fonović, M. Bogoy, *Expert Rev. Proteomics* **2008**, *5*, 721–730; c) J. Clerc, B. I. Florea, M. Kraus, M. Groll, R. Huber, A. S. Bachmann, R. Dudler, C. Driessen, H. S. Overkleeft, M. Kaiser, *ChemBioChem* **2009**, *10*, 2638–2643; d) D. A. Shannon, C. Gu, C. J. McLaughlin, M. Kaiser, R. A. van der Hoorn, E. Weerapana, *ChemBioChem* **2012**, *13*, 2327–2330; e) F. Zou, M. Schmon, M. Sienczyk, R. Grzywa, D. Palesch, B. O. Boehm, Z. L. Sun, C. Watts, R. Schirmbeck, T. Burster, *Anal. Biochem.* **2012**, *421*, 667–672; f) H. Y. Hu, D. Vats, M. Vizovisek, L. Kramer, C. Germanier, K. U. Wendt, M. Rudin, B. Turk, O. Plettenburg, C. Schultz, *Angew. Chem. Int. Ed.* **2014**, *53*, 7669–7673; *Angew. Chem.* **2014**, *126*, 7802–7806.
- [35] L. E. Sanman, M. Bogoy, *Annu. Rev. Biochem.* **2014**, *83*, 249–273.
- [36] a) L. I. Willems, H. S. Overkleeft, S. I. van Kasteren, *Bioconjugate Chem.* **2014**, *25*, 1181–1191; b) P. Yang, K. Liu, *ChemBioChem* **2015**, *16*, 712–724.
- [37] J. Oleksyszyn, L. Subotkowska, P. Mastalerz, *Synthesis* **1979**, 985–986.
- [38] Ł. Winiarski, J. Oleksyszyn, M. Sieńczyk, *J. Med. Chem.* **2012**, *55*, 6541–6553.
- [39] A. Belyaev, X. Zhang, K. Augustyns, A. M. Lambeir, I. De Meester, I. Vedernikova, S. Scharpé, A. Haemers, *J. Med. Chem.* **1999**, *42*, 1041–1052.
- [40] M. Skoreński, J. Oleksyszyn, M. Sieńczyk, *Tetrahedron Lett.* **2013**, *54*, 4975–4977.
- [41] M. D. Mertens, J. Schmitz, M. Horn, N. Furtmann, J. Bajorath, M. Mareš, M. Gütschow, *ChemBioChem* **2014**, *15*, 955–959.
- [42] B. Boduszek, J. Oleksyszyn, C. M. Kam, J. Selzler, R. E. Smith, J. C. Powers, *J. Med. Chem.* **1994**, *37*, 3969–3976.
- [43] B. Lejczak, P. Kafarski, J. Szewczyk, *Synthesis* **1982**, 412–414.
- [44] a) E. Parisini, P. Metrangolo, T. Pilati, G. Resnati, G. Terraneo, *Chem. Soc. Rev.* **2011**, *40*, 2267–2278; b) L. A. Hardegger, B. Kuhn, B. Spinnler, L. Anselm, R. Ecabert, M. Stihle, B. Gsell, R. Thoma, J. Diez, J. Benz, J. M. Plancher, G. Hartmann, D. W. Banner, W. Haap, F. Diederich, *Angew. Chem. Int. Ed.* **2011**, *50*, 314–318; *Angew. Chem.* **2011**, *123*, 329–334; c) R. Wilcken, M. O. Zimmermann, A. Lange, A. C. Joerger, F. M. Boeckler, *J. Med. Chem.* **2013**, *56*, 1363–1388; d) J. Ren, Y. He, W. Chen, T. Chen, G. Wang, Z. Wang, Z. Xu, X. Luo, W. Zhu, H. Jiang, J. Shen, Y. Xu, *J. Med. Chem.* **2014**, *57*, 3588–3593.
- [45] a) J. A. Bertrand, J. Oleksyszyn, C. M. Kam, B. Boduszek, S. Presnell, R. R. Plaskon, F. L. Suddath, J. C. Powers, L. D. Williams, *Biochemistry* **1996**, *35*, 3147–3155; b) E. Burchacka, M. Zdzalik, J. S. Niemczyk, K. Pustelny, G. Popowicz, B. Władyska, A. Dubin, J. Potempa, M. Sienczyk, G. Dubin, J. Oleksyszyn, *Protein Sci.* **2014**, *23*, 179–189.
- [46] B. Walker, S. Wharry, R. J. Hamilton, S. L. Martin, A. Healy, B. J. Walker, *Biochem. Biophys. Res. Commun.* **2000**, *276*, 1235–1239.
- [47] M. Frizler, M. D. Mertens, M. Gütschow, *Bioorg. Med. Chem. Lett.* **2012**, *22*, 7715–7718.
- [48] a) T. Murase, T. Yoshihara, K. Yamada, S. Tobita, *Bull. Chem. Soc. Jpn.* **2013**, *86*, 510–519; b) D. Häußler, M. Gütschow, *Synthesis* **2016**, 245–255.
- [49] a) T. Terai, T. Nagano, *Curr. Opin. Chem. Biol.* **2008**, *12*, 515–521; b) P. W. Elsinghorst, W. Härtig, S. Goldhammer, J. Grosche, M. Gütschow, *Org. Biomol. Chem.* **2009**, *7*, 3940–3946; c) R. S. Agnes, F. Jernigan, J. R. Shell, V. Sharma, D. S. Lawrence, *J. Am. Chem. Soc.* **2010**, *132*, 6075–6080; d) O. Vázquez, M. I. Sánchez, J. L. Mascareñas, M. E. Vázquez, *Chem. Commun.* **2010**, *46*, 5518–5520; e) S. Nizamov, K. I. Willig, M. V. Sednev, V. N. Belov, S. W. Hell, *Chem. Eur. J.* **2012**, *18*, 16339–16348; f) L. Meimeitis, J. C. Carlson, R. J. Giedt, R. H. Kohler, R. Weissleder, *Angew. Chem. Int. Ed.* **2014**, *53*, 7531–7534; *Angew. Chem.* **2014**, *126*, 7661–7664; g) F. Kohl, J. Schmitz, N. Furtmann, A. C. Schulz-Fincke, M. D. Mertens, J. Küppers, M. Benkhoff, E. Tobiasch, U. Bartz, J. Bajorath, M. Stirnberg, M. Gütschow, *Org. Biomol. Chem.* **2015**, *13*, 10310–10323.

Received: January 15, 2016

Published online on May 23, 2016